Analysis of Exhaust and Stack Systems of a Warship

Seyfettin Bayraktar*, Aykut Safa, Uğur Buğra Çelebi, Serkan Ekinci

Department of Naval Architecture, Yildiz Technical University, Istanbul, 34349, Turkiye

Abstract Unlike the commercial vessels, diesel and gas turbine engines are frequently utilized in warships, even both, CODOG (Combined Diesel or Gas Turbine Engine System). In this study, a warship diesel exhaust system with CODOG propulsion is analyzed analytically and then compared with the numerical results obtained by a CFD code of FLUENT. The pressure losses due to a lot of number of parameters such as friction, bending, etc. are calculated with respect to the design rules document given for warship exhaust systems. The flow analysis of system is performed in 2-D model with full scale and velocity vectors, pressure and temperature fields are obtained through simulation.

In the analysis, the diesel exhaust system with two-inlet pipes and one outlet is considered. The pressures at inlets and outlet are calculated via CFD code of FLUENT and results are compared with analytical calculations and proved that the total pressure loss is within the maximum pressure limit permitted by diesel engine manufacturer.

1. Introduction

The function of an engine intake and exhaust system is to deliver air into the engine and dispose of the engine exhaust with as little impact as possible on engine performance [1]. Major system components of an engine exhaust system are particulate removal filters, exhaust silencers and exhaust duct system components. Common materials for duct system and duct system components are carbon steel and another is stainless steel.

In this study, engine exhaust duct components are of two exhaust ducts; unite in one duct system of compensator modeled as a straight duct, diffuser and 90° bend, respectively. In engine silencer manuals, pressure drops of 5-10 mbar are suggested [2]. For flow continuity, sudden or slow expansions are necessary and effects of negative pressure through the components are to be observed.

Diesel engine manufacturers suggest 50 mbar pressure drops, approximately. The majority of the pressure drop is produced while the exhaust gases passing through entrance zone and later in the compensators and bends, at gross.

In this study, diesel exhaust system is taken into account to analyze temperature, velocity and, in particular, pressure losses. The results evaluated by CFD are compared with analytical calculation. It is seen that, although the pressure losses found by CFD is much higher (about five times) than found by analytical calculations, it is below the maximum limit allowed by diesel engine manufacturer [2].

2. Numerical

In this paper, a component of warship main propulsion system, exhaust system of a CODOG plant is investigated by using computational fluid dynamics (CFD) and pressure losses found by simulation are compared with analytical results.

For the simulation, a warship propelled with CODOG system is taken into account and pressure losses calculations is done according to USA Naval Force Warship Engineering Department rules [3]. In these calculations, all the parts of the exhaust system (inlet, pipe, diffuser, nozzle and bends) are taken into account. As it is well known that velocity, temperature, density and dynamic viscosity and friction factor affect pressure losses.

ISSN - 1223-7221
© 2006 Ovidius University Press

All this parameters, above, are taken into account in the simulation and analytical calculations. And, simulation is performed by using one of the commercially available CFD codes, FLUENT®. The dimensions of the system are shown in Fig. 1.

In the CFD simulation, GAMBIT® pre-processor of the FLUENT generates the geometry and meshes. During the mesh generation the boundary layer meshes are applied according to Eq.1 and Eq.2 for obtaining more accurate results.

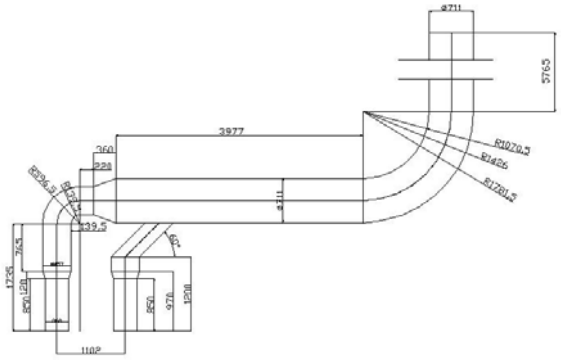

Fig. 1: The geometry and dimensions of the exhaust system.

$$\mathrm{Re}_L = \frac{U_{in} L}{\nu_{fluid}} \tag{1}$$

$$\delta_{bl} = \frac{0.38L}{\mathrm{Re}_L^{1/5}} \tag{2}$$

In the above equations, U_{in} is pipe inlet velocity, L length of the pipe, υ_{fluid} dynamic viscosity of the fluid flowing into pipe and Re_L is the Reynolds number at the distance of the L, while δ_{bl} is the boundary layer at L. Table 1 shows the values used in the boundary layer calculation and mesh generation.

Table 1: Input data for the boundary layer mesh calculations.

U_{in} (m/s)	L (m)	υ_{fluid} (m^2/s)	Re_L	δ_{bl} (mm)
104	4	1.10^{-05}	$41.6\ 10^{06}$	45.5

As can be seen from Table 1, the calculated maximum boundary layer along the pipe is found 45.5 mm for the maximum length of the pipe. For boundary layer mesh, the height of the first row of the boundary layer is chosen 0.024 mm and growing ratio is 20% for the 33 row. This number of the rows provides totally about 49 mm boundary layer thickness. Applying boundary layer mesh in this way provides us to dispose 33 rows of mesh into boundary layer in the CFD calculation.

For the whole geometry, 382500 quadrilateral cells are used and this gives 385351 nodes in the domain (Fig. 2). The maximum skew of the mesh elements is found 0.34 for only 0.03% of the used cells and such a skew is acceptable. In Fig. 2 meshes in only bend region are showed. It is well known that CFD results depend very upon the grid number used in the calculation. Coarse meshes give wrong results, while very fine meshes increase iteration time and costs. So a grid independence study is done with approximately 1500000 mesh elements and it is seen that 382500 quadrilateral cells are fine enough for this simulation.

For the mathematical model, time-averaged steady-state mean flow equations of continuity, momentum and energy can be written in Cartesian tensor notation follows:

$$\frac{\partial U_i}{\partial x_i} = 0 \tag{3}$$

$$\rho \frac{DU_i}{Dt} = -\delta_{ij} \frac{\partial P}{\partial x_j} + \mu \frac{\partial^2 U_i}{\partial x_j^{\ 2}} \tag{4}$$

$$\frac{DT}{Dt} = \alpha \nabla^2 T \tag{5}$$

As turbulence model, the Standard k-ε turbulence model of Launder and Spalding [4] has been used. The corresponding turbulence equations are given in Eq. 6 for turbulence kinetic energy and in Eq. 7 for turbulence kinetic energy dissipation rate.

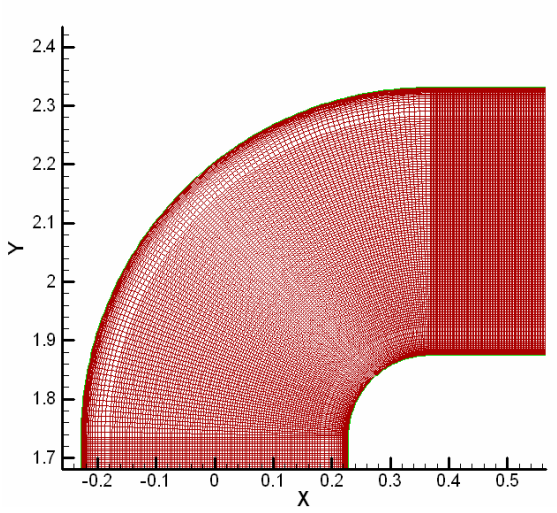

Fig. 2: Mesh structure of the diesel exhaust system

$$\rho\frac{Dk}{Dt}=\frac{\partial}{\partial x_i}\left[\left(\mu+\frac{\mu_t}{\sigma_k}\right)\frac{\partial k}{\partial x_i}\right] \qquad (6)$$
$$+G_k+G_b-\rho\varepsilon-Y_M$$

$$\rho\frac{D\varepsilon}{Dt}=\frac{\partial}{\partial x_i}\left[\left(\mu+\frac{\mu_t}{\sigma_\varepsilon}\right)\frac{\partial \varepsilon}{\partial x_i}\right] \qquad (7)$$
$$+C_{1\varepsilon}\frac{\varepsilon}{k}\left(G_k+C_{3\varepsilon}G_b\right)-C_{2\varepsilon}\rho\frac{\varepsilon^2}{k}$$

$C_{1\varepsilon}, C_{2\varepsilon}$ and $C_{3\varepsilon}$ coefficients are set equal to 1.44, 1.92 and 0.09, respectively. $\sigma_k = 1.0$ and $\sigma_\varepsilon = 1.3$ are the turbulent Prandtl numbers for k and ε, respectively. G_k represents the generation of turbulent kinetic energy due to the mean velocity gradients. G_b is the generation of turbulent kinetic energy due to buoyancy. Y_M represents the contribution of the fluctuating dilatation in compressible turbulence to the overall dissipation rate. In the near wall region, molecular viscosity affects the level of turbulence energy, so the standard k-ε model is not applicable near the solid walls. To handle the standard near wall flow, near-wall function of Launder and Spalding [4], which uses linear and logarithmic laws to describe the velocity profile near the wall, is used. In FLUENT code [5] the governing equations are discretized using second order upwind interpolation scheme, and the discretized equations are solved using SIMPLEC algorithm. Typical relaxation factors used here is 0.3, 0.7 and 0.8 for pressure, momentum and turbulence kinetic energy and turbulence dissipation rate. For both energy and turbulent viscosity, the relaxation factor is 1, The solution is considered to be converged, when the normalized energy residual is lower than 10^{-6} and normalized residuals of all the other variables are below 10^{-5}.

3. Analytical

The analytical calculations for this exhaust system are performed in guidance of Ref. [3]. In calculations the Mach number of the flowing into the exhaust pipes is taken as less than 0.3, so, the fluid flow for the case can be considered as incompressible.

As can be seen from Fig. 1, the exhaust system has two-inlet pipes and one outlet. In the analytical calculations, the inlet mass flow rate is taken as half of the total mass flow rate of the diesel engine. The pressure loss in the exhaust system is calculated as shown in Eq. 8 in general form.

$$\Delta P = (q+p)_{inlet} - (q+p)_{outlet} \qquad (8)$$

Here q represents the dynamic pressure while p stands for static pressure.

The pressure losses for straight pipes:

$$\Delta p_{\text{compressible}} = \Delta p_{\text{incompressible}}.\ C_f$$

$$\Delta p_{\text{incompressible}} = f\frac{L}{d}\frac{V^2}{2g} = f\frac{L}{d}q \qquad (9)$$

In this equation;
V: Fluid velocity
f: Friction coefficient
L: Straight pipe length
d: Straight pipe diameter

q: Dynamic pressure ($V^2/2g$)
g: Acceleration of gravity
C_f: Correction factor regarding Mach number, straight pipe length, straight pipe diameter and friction coefficient.

The pressure losses at bends:
The pressure losses at bends depend on a lot of flow and geometrical parameters. Efficiency losses coefficient ($K_{efficient}$) includes all these parameter effects. $K_{efficient}$ is obtained by correction coefficient factor (K), which used for standard cases [3].

$$K_{efficient} = K .(C_{LM}.C_{LD}.C_{Re}.C_M.C_{h/l}.C_{\Delta A}.C_S.C_i)$$

$$\Delta p = q\left[K_{efficient} + \left(\frac{A_i}{A_o}\right)^2 - 1\right] \qquad (10)$$

C_{LM}: Correction coefficient for upstream.
C_{LD} : Correction coefficient for downstream.
C_{Re} : Correction coefficient for Reynolds number.
C_M : Compressibility correction coefficient.
$C_{h/l}$: Height/Length correction coefficient.
$C_{\Delta A}$: Cross-section area change coefficient
C_S : Pipe or flow split correction coefficient
C_i : Flow correction coefficient for entry bend.

The pressure losses for diffusers:

In conventional diffusers are used to decrease the flow velocity by increasing the cross-section area of the geometry. In diffusers the static pressure increases since conventional diffusers are used. Flow velocity can be decreased with increasing cross-section area of the geometry. Therefore, as a consequence, the static pressure increases.

$$\Delta p = \left\{\left(1 - \frac{A_i}{A_o}\right)^2 - \left[1 - \left(\frac{A_i}{A_o}\right)^2\right]\right\} q \qquad (11)$$

$\frac{A_i}{A_o}$: Inlet and outlet areas for fluid flow.

4. Results and Discussions

The main goal of this paper is to show the CFD capability for such a problem. After 72 hours simulation time the equations are converged. The velocity vectors, temperature, turbulence kinetic energy and pressure fields are obtained and pressure losses found by CFD and analytical calculations are compared, In Fig. 3, it is seen that after the bends the lower pressure regions occurs due to recirculation as seen in Fig. 4 and in Fig. 7.

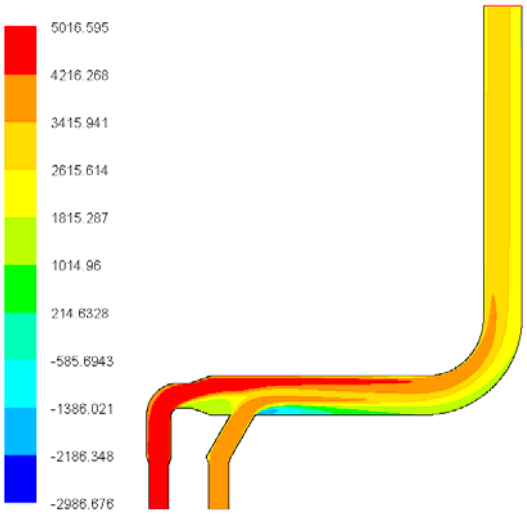

Fig. 3: The contours of total pressure field (Pa).

The similar recirculation region is also developed after the second bend. The existence of such recirculation regions causes to noise and vibration, so, it is suggested that extra insulation must be provided regarding these regions. It is also supported by turbulence kinetic energy plot (Fig. 6).

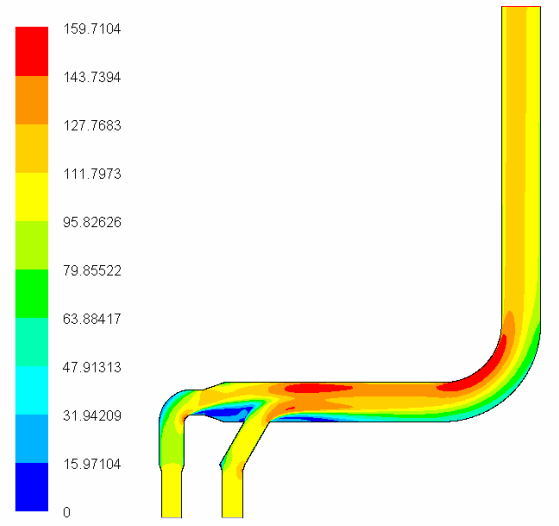

Fig. 4: The contours of velocity field (m/s).

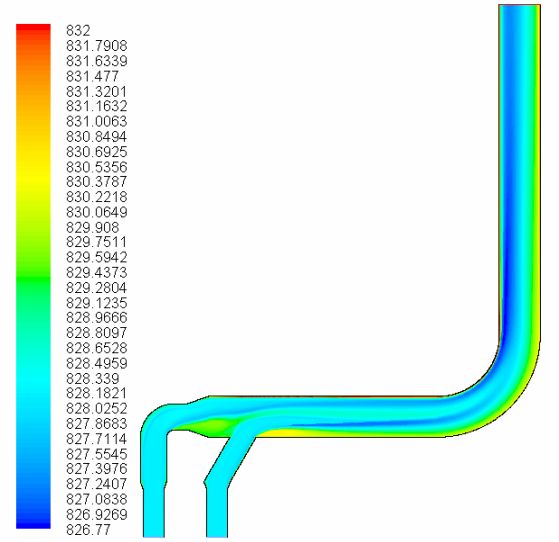

Fig. 5: The contours of total temperature field (K).

The temperature distribution in exhaust system can be seen in Fig. 5. In this figure it is observed that the hot inlet gaseous is getting cooler towards to exhaust system outlet. But it must be added that the second bend stands as a obstacle for the first bend so the flowing fluid near the second bend side could not be cooled enough. To achieve a full cooling operation some improvements must be done especially near those regions.

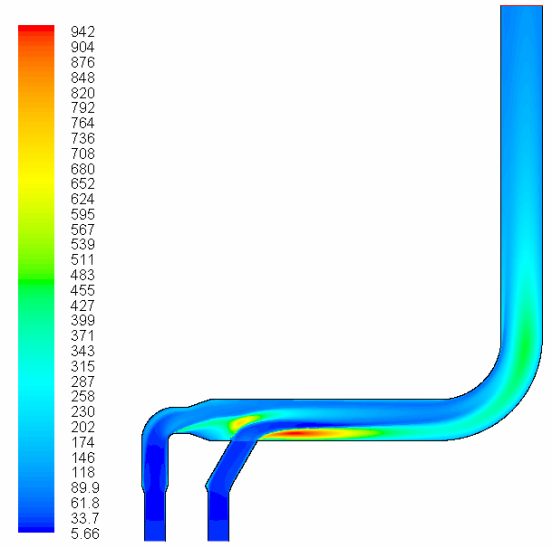

Fig. 6: The contours of turbulence kinetic energy ($Km^2/s^{2)}$.

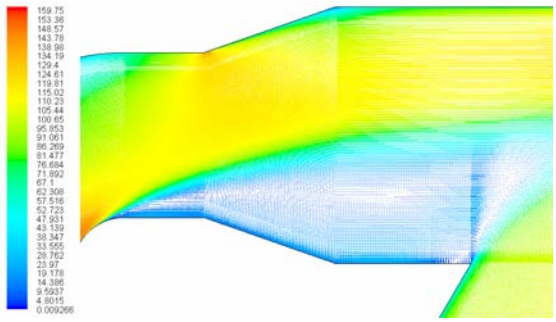

Fig. 7: The velocity vectors after the first bend.

In CFD study, the pressure calculations are obtained via FLUENT code. As can be seen from Table 1, the maximum outlet pressure is found 3000 Pa while inlet pressure is about 4500 Pa. The pressure losses in analyzed exhaust system are calculated as differences between inlet and outlet maximum pressures. In the analytical calculations the exhaust system inlet pressure is taken as diesel engine outlet pressure as given in [2].

Table 2: Analytical and CFD results

CFD RESULTS			ANALYTICAL RESULTS			Maximum Pressure Losses Limit Allowed by Producer [2]
Maximum Outlet Pressure (Pa)	Maximum Inlet Pressure (Pa)	$\Delta P=P_{inlet}-P_{outlet}$ (Pa)	Outlet Pressure (Pa)	Inlet Pressure (Pa)	ΔP (Pa)	ΔP (Pa)
≅3000	*≅4500*	*≅1500*	*≅900*	*≅1200*	*300*	*5000*

The outlet pressure is calculated as explained in Ref. [6] in detail. The difference between inlet and outlet maximum pressures is found 300 Pa. Although there are difference between CFD and analytical results, the maximum pressure losses found by CFD is much lower than the limit pressure differences given by diesel engine producer.

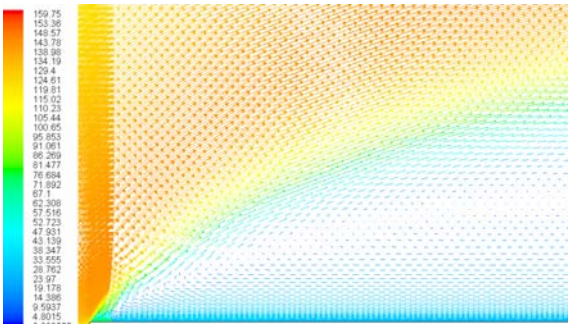

Fig. 8: The velocity vectors after the second bend.

4. Conclusion

In the present paper, the CFD and analytical calculations of a warship in service of Turkish Naval Force is examined and obtained results are compared each other. After the comparison, it is seen that pressure losses found by analytical calculations found very lower than the CFD results but these CFD results are lower than maximum pressure losses permitted by diesel engine producer. As conclusion, it is showed that the computational fluid dynamics calculations can be used in such a practical problem. Regarding to the presence of the recirculation regions occurring after the bends, extra insulation is suggested for the region.

5. Acknowledgments

The authors thank Orhan Barbaros Okan for useful help and discussions.

6. References

* E-mail address: sbay@yildiz.edu.tr

[1] M.A. Gîrțu and A.J. Epstein, Army TM 5-692-2, *Maintenance of Mechanical and Electrical Equipment at Command, Control, Communications, Computers, Intelligence, Surveillance, and Reconnaissance (C4ISR) Facilities*, Departments of the Army (CEMP-SP).

[2] MTU Technical Project Guide, *Main Propulsion Plans with MTU Series 396TE/TB.4, Diesel Engines VPS07 201* (51 1E), 1/94, 1994.

[3] NSEC, *Data for Estimating Pressure Losses in Engine and Boiler Inlet and Exhaust Systems, DDS 221-1*. Department of the Navy Ship Engineering Center, 1972.

[4] B.E. Launder, D.B. Spalding, *Comp. Methods* Appl. Mech. Eng., Vol.3, pp.269.

[5] FLUENT Manuals, 2004.

[6] Okan, O. B., "I*nvestigation of Exhaust and Stack Systems of Warships*", Msc Thesis, Yildiz Technical University, 2005, (in Turkish)